Shape optimization of Reactive mufflers using Threshold Acceptance and FEM Methods

Abdelkader Khamchane*[1], Youcef Khelfaoui †[1], Brahim Hamtache ‡[1]

[1] Laboratoire de Mécanique, Matériaux et Energétique (L2ME), Université de Bejaia, Faculté de Technologie Targa ouzemour Bejaia, DZ 06000, Algeria

Résumé

L'optimisation de forme des silencieux réactifs sous contrainte d'espace a une grande importance dans la conception d'environnements moins bruants. Dans ce travail, les performances acoustiques de trois types de silencieux soumis à un espace limité sont étudiées. Une analyse d'optimisation de forme est effectuée en utilisant un algorithme d'optimisation appelé Threshold Acceptance (TA). La conception optimale obtenue est analysée par la méthode des éléments finis (FEM : Finit Element Method). Cette approche numérique est basée sur la maximisation de la perte de transmission acoustique (STL : Sound Transmission Loss) à l'aide de la méthode de transfert de matrices (TMM : Transfer Matrix Method) qui est une méthode de modélisation basée sur le modèle de propagation d'onde plane. La solution en élément finis utilisée pour analyser la STL est basée sur la méthode de puissance acoustique, un code de calcul standard utilisé pour analyser en 3D l'atténuation acoustique des silencieux par la méthode FEM. La capacité acoustique des silencieux obtenus est évaluée en comparant la solution FEM à la méthode analytique. Les résultats montrent que la valeur maximale de la STL est précisément située à la tonalité ciblée. En outre, la performance acoustique du silencieux avec tube à l'entrée et à la sortie prolongée se trouve être supérieure aux autres types de silencieux. Par conséquent, cette approche fournit un schéma rapide pour l'optimisation de la forme des silencieux réactifs.

Mots clefs : silencieux réactifs, algorithme d'optimisation, méthode de transfert de matrices, puissance acoustique

Abstract

The shape optimization of reactive muffler under space constraint becomes of great importance in the design of quieter environments. In this paper, the acoustical performance of three different expansion-chamber mufflers with extended tube under space constraint is presented. A shape optimization analysis is performed using a novel scheme called Threshold Acceptance (TA). The best design obtained by the shape optimization method is analyzed by Finite Element Method (FEM). This numerical approach is based on the maximization of the Sound Transmission Loss (STL) using the Transfer Matrix Method (TMM). The TMM method is a modelling method based on the plane wave propagation model whereas the FEM solution is based on the acoustical power method. A standard computational code is used to analyze the sound attenuation of the mufflers by the FEM method in 3D. The acoustical ability of the mufflers is than assessed by comparing the FEM solution with the analytical method. Results show that the maximal STL is precisely located at the desired targeted tone. In addition, the acoustical performance of muffler with inlet and outlet extended tube is found to be superior to the other ones. Consequently, this approach provides a quick scheme for the shape optimization of reactive mufflers.

Keywords: reactive muffler, threshold acceptance, transfer matrix method, sound acoustic power

1 Introduction

The use of mufflers for exhaust noise attenuation with limited space in vehicles and machinery pushes the researchers to develop different numerical modelling methods [1-2]. The most common type of linear acoustic model applies classical electrical filter theory. This theory is widely known as the transfer matrix method (TMM) [3]. Though, it is also referred to as the 4-pole parameter method [4-6]. A technique that combines the use of transfer matrix approach and finite element method in the study of duct acoustics is reported after by Craggs in 1989 [7].

Since the muffler space dimension is often limited to meet the demands of operation and maintenance, there are increasing interests in designing mufflers in order to optimize the STL using shape optimization methods [8]. A simple expansion chamber muffler is studied by Bernhard [9] by using a shape optimization method with a non-constrained space condition. To obtain a good acoustical performance for the shape optimization of mufflers, novel schemes have appeared such as Genetic Algorithm (GA) and Simulating Annealing (SA) [10]. Yeh and al. [11] studied the shape optimal design of a double expansion-chamber muffler under space constraints by using SA and GA optimizers. Their study reveals that either SA or the GA is applicable in the optimization analysis. Both algorithms are much easier to use compared to gradient-based optimizers which require a good starting.

*abdelkader.khamchane@yahoo.fr
†youcef.khelfaoui@yahoo.fr
‡ brahim.hamtache@yahoo.fr

This paper is built on the acoustic attenuation study of three types of expansion-chamber mufflers with extended tubes under space constraints by using a deterministic acceptance criterion optimizer named Threshold Acceptance combined with a finite element analysis.

2 Mathematical models

The reactive mufflers adopted for the noise reduction in this work are composed of three types of inlet/outlet extended tube mufflers as shown in figure 1 (a, b and c). The three kinds of mufflers are left inlet extended tube, right outlet extended tube and inlet/outlet extended tube. The different acoustical elements of the mufflers (acoustic pressure *p* and acoustic particle velocity *u*) are illustrated in figure 2 (a, b and c). These elements within the left and right extended tube mufflers are represented by seven nodes and for the inlet and outlet extended tube muffler are represented by eight nodes.

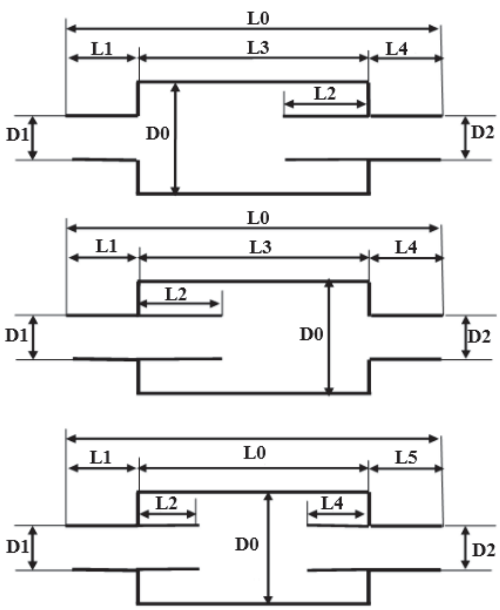

Figure 1: Sketches of expansion-chamber mufflers with extended tube: (a) inlet, (b) outlet, (c) inlet & outlet side.

Two different approaches were used to analyze the acoustical performance of the three mufflers under chosen limited space (L= 1.5 m, D0 = 0.3). These approaches are the sound acoustic power and the transfer matrix methods. The most widely used acoustical performance to characterize the sound attenuation of the mufflers is the sound transmission loss (STL). This value depends only on the muffler and not on the sound source. It is considered as the best parameter to use when comparing different methods and designs [12]. The optimization method is developed using Matlab tool. For the FEM and simulation analysis a standard computational code named COMSOL Multiphysics Tools is used.

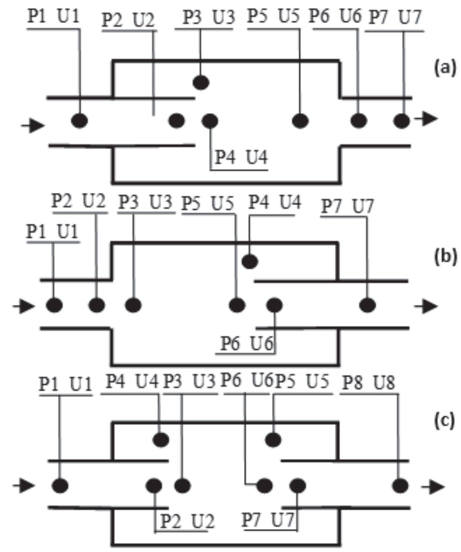

Figure 2: Sketches of the one-dimensional plane wave propagation of expansion-chamber mufflers with extended inlet/outlet tube: (a) inlet, (b) outlet, (c) inlet & outlet side.

3 Numerical assessment

3.1 Shape optimization method

A system of four-pole matrix evaluating the acoustical performance (sound transmission loss) is used and derived by using a decoupled numerical method called Transfer Matrix Method (TMM). This method uses 2 x 2 matrices to relate two variables at planes on either side of an acoustic component. The matrices for individual components can be readily combined to form a single and overall matrix that describes the behavior for a multi-component muffler's system [5, 13].

A Threshold Acceptance method, a deterministic acceptance criteria optimizer similar to simulated annealing, is applied to the optimizations of the mufflers.

3.2 Theoretical formulation

The acoustical system of four-pole matrix uses 2 x 2 matrix to relate two variables at planes (acoustic pressure (*p*) and volume velocity (*u*)) on either side of an acoustic component [14, 15]. To describe the overall acoustic property of the muffler we need to relate all the individual matrices in one total transfer matrix of the system as:

$$T = T_1\, T_2\, T_3 \ldots \tag{1}$$

The following general transfer matrix may be written to relate the state variables of straight duct and expansion/contracted ducts respectively for the three kinds of expansion-chamber mufflers with extended tube.

$$T_i = e^{-j\frac{M_i k L_i}{\left(1-M_i^2\right)}} \begin{bmatrix} \cos\left(\frac{kL_i}{1-M_i^2}\right) & j\sin\left(\frac{kL_i}{1-M_i^2}\right) \\ j\sin\left(\frac{kL_i}{1-M_i^2}\right) & \cos\left(\frac{kL_i}{1-M_i^2}\right) \end{bmatrix} \quad (2)$$

$$T_i^{'} = \begin{bmatrix} 1 & 1 \\ 1 & \frac{S_i}{S_{i-1}} \end{bmatrix} \quad (3)$$

Where T_i , T'_i , M, k, L, S, j and i are respectively the transfer matrix of straight ducts, the transfer matrix of expansion/contracted ducts, the Mach number, the wave number, the length of element, the area of the element, the imaginary unit section and the i represent the i[th] node.

For the cross-sectional discontinuity case, the transition elements used are shown in the first column of table 1. By using decreasing element-subscript values with distance from the noise source, the cross-sectional areas upstream and downstream of the transition (S_3, S_2 and S_1) are related through:

$$C_1S_1 + C_2S_2 + S_3 = 0 \quad (4)$$

The constants C_1 and C_2 are selected to satisfy the compatibility of the cross-sectional areas across the transition.

Table 1: Parameters values of transition elements

Element Type	C_1	C_2	K
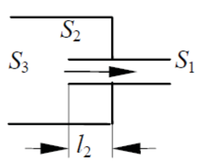	-1	-1	$\frac{1-\frac{S_1}{S_3}}{2}$
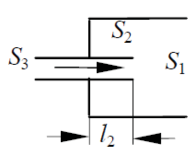	-1	1	$\left(\frac{S_1}{S_3}-1\right)^2$

Table 1 also shows the pressure loss coefficient K for each configuration that accounts for conversion of some mean-flow energy and acoustical field energy into heat at the discontinuities. As indicated, $K \leq 0.5$ for area contraction, while $K \rightarrow (S_1 / S_3)^2$ for area expansions at large values of S_1 / S_3.

The four-pole matrices of the ducts with cross-sectional discontinuities [15] (for Mach number M = 0) is given by

$$T_{discontinuitate} = \begin{bmatrix} 1 & 0 \\ \frac{C_2}{C_1\left(-j\frac{c_0}{S_2}\cot kl\right)} & 1 \end{bmatrix} \quad (5)$$

The computation of the transfer matrix for the whole silencer is achieved based on the individual matrices which relate the pressure P and mass velocity V at the inlet and outlet. The individual matrices are calculated separately for every sector as:

$$\begin{pmatrix} p_i \\ \rho_0 c_0 u_i \end{pmatrix} = \begin{bmatrix} T_{11} & T_{12} \\ T_{21} & T_{22} \end{bmatrix} \begin{pmatrix} p_o \\ \rho_0 c_0 u_o \end{pmatrix} \quad (6)$$

Where T_{11}, T_{12}, T_{21} and T_{22} are referred to as the four poles of the acoustical system. The STL of a muffler is calculated as [5]:

$$STL\left(f, Q, R_1, R_2, R_3, R_4\right) = 20\log\left[\left[\frac{Y_n}{Y_1}\right]^{1/2}\left|\frac{T_{11} + T_{12}Y_n + T_{21}Y_1 + T_{22}(Y_1/Y_n)}{2}\right|\right] \quad (7)$$

Y_1 is calculated for the input pipe and Y_n for the output pipe. Where for the inlet and outlet mufflers:

$R_1=D_1/D_0$, $R_2=D_2/D_0$, $R_3=L_3/L_0$, $R_4=L_2/L_0$, $L_1=1/2(L_0-L_3)$, $L_4=1/2(L_0-L_3)$, $L_0=L1+L3+L5$.

And for Inlet and outlet muffler:

$R_1=D_1/D_0$, $R_2=D_2/D_0$, $R_3=L_3/L_0$, $R_4=L_6/L_0$, $L_1=1/2(L_0-L_3)$, $L_5=1/2(L_0-L_3)$, $L_2=1/2(L_3-L_6)$, $L_0=L1+L3+L5$

Because of the remarkably pure tone noise effect at 300 Hz [11], noise elimination at this frequency by shape optimization is applied.

3.3 Threshold Acceptance

Threshold Acceptance method applied in this work is a metaheuristic algorithm. It's a modification of the well-known Simulated Annealing metaheuristic method (SA) [16]. The SA method draws its analogy from the annealing process of solids. The solid is heated to a high temperature and gradually cooled in order to crystallize. It must be cooled slowly such that the atoms have enough time to align themselves to reach a minimum energy state. This analogy can be used in combinatorial optimizations with the states of the solid corresponding to the feasible solution. The energy at each state correspond to the value of objective function and the minimum energy represent the optimal solution [17].

SA always accepts moves to neighboring solutions that improve the objective function value. More precisely, the solution (S) in the neighborhood $N(S)$ is accepted as the new current solution if $\Delta \leq 0$, where $\Delta = C(S')-C(S)$ in which C denotes the objective function. To allow the search to escape a local optimum, a stochastic approach is used to direct the search. A move that worsens the objective function value is accepted with a probability $e^{-\Delta/T}$ if $\Delta > 0$. T is a parameter called the Temperature.

The value of T varies from a relatively large value to a small value close to zero. An initial temperature and an optimization temperature are chosen in this interval at each step of optimization of the algorithm. This method of temperature selection is identical to that of the metal cooling process.

The TA algorithm uses a predetermined deterministic sequence to decide whether a new point is selected or not (if worse than the current point), whereas SA method probabilistically determines a new point selection at every iteration.

Dueck and Scheurer [18] simplified the SA procedure by leaving out the probabilistic element in accepting worse solutions. Instead, they introduced a deterministic threshold (τ) and a worse solution is accepted if its difference to the incumbent solution is smaller or equal to the threshold. The new procedure is named Threshold Acceptance.

The key components of TA are the function *g(t)* that determines the lowering of the threshold during the course of the procedure, the stopping criteria as well as the methods used to create initial and neighboring solutions. The main advantages of TA are its conceptual simplicity and its excellent performance on different combinatorial optimization problems [19].

3.4 FEM Analysis method

In the second part of this paper, we analyze the acoustical performance of the obtained shape optimized mufflers by using FEM. The available numerical tool used for analyzing muffler performance includes 3D linear acoustic codes with and without mean flow is using FEM methods where the most important effect of flow is included by altering the boundary conditions without considering the mean flow [20].

The following equation defines the attenuation d_w (dB) of the acoustic energy is:

$$d_w = 10 \log\left(\frac{w_0}{w_i}\right) \tag{8}$$

Here w_0 and w_i denote the outgoing power at the outlet and the incoming power at the inlet respectively. Each of these quantities can be calculated as an integral over the corresponding surface:

$$w_0 = \int_{\partial\Omega} \frac{|p|^2}{2\rho c_s} dA \tag{9}$$

$$w_i = \int_{\partial\Omega} \frac{p_0^2}{2\rho c_s} dA \tag{10}$$

The FEM model solves the problem in the frequency domain using the time-harmonic pressure of the acoustic application mode. The STL is calculated directly with the computational code tool using the acoustic power method at the inlet and at the outlet of the acoustic system. Each model of muffler is simulated using a three dimensional model and is meshed using the Lagrange-quadratic elements. A harmonic pressure of $1Pa$ is specified at the inlet of the muffler and a radiation boundary condition is applied at the inlet and outlet of the muffler. A material with default values of air is created with density of 1.2 kg/m3 and with sound speed of 340 m/s. By using the default values of air, the acoustic damping is not taken into account.

3.5 Case studies

To check the transmission loss model on the single inlet chamber muffler a comparison between theoretical and experimental data [3] is realized. As shown in figure 3, there is a coherence between the theoretical and experimental data. Hence, the transmission loss model is acceptable and can be applied to the studied models.

The available space selected for the mufflers is 0.5 m in width 0.5 m in height and 1.5 m in length. To obtain the best acoustical performance within a fixed space a pure tone noise with 300 Hz is applied for the mufflers as a numerical case. Also to reach an initial transition probability of 0.5 of the TA method, the initial temperature is selected as 0.2 and the flow rate (Q = 0.01 (m3/s)) is preset in advance to simplify the optimization for the mufflers [10]. The selected space constraints ranges for the three types of mufflers are:

R_1: [0.1, 0.5], R_2: [0.1, 0.5], R_3: [0.2, 0.8] and R_4: [0.2, 0.8]

After shape optimization of the mufflers, a numerical analysis by FEM is presented in the second part of this work. To assess the acoustical performance of each idealized muffler a 3D simulation analysis is applied for the FEM. The used parametric solver provides results for a range of frequencies. The software computes integrals in the power expressions using boundary integration coupling variables and it plots the resulting attenuation versus frequency.

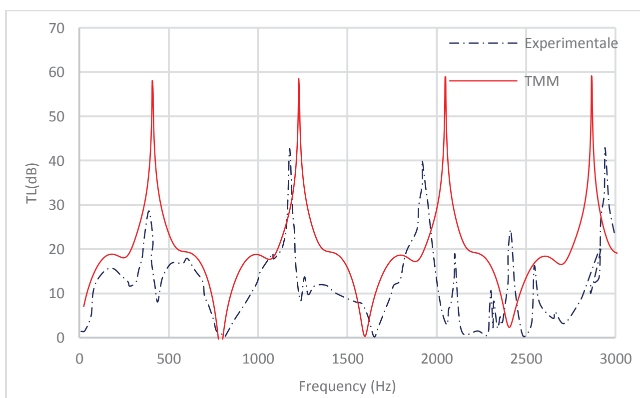

Figure 3: Performance curves of STL, comparison between TMM theoretical model and experimental values of simple expansion chamber muffler with extended tube [3].

3.6 Objective Function

The accuracy of the TA optimization depends on two control parameters: the cooling rate (CR) and the number of iteration (I_{max}). The optimization process with respect to objective functions (*Obj1, Obj2* and *Obj3*) is performed by varying these parameters. From formula (7), the objective functions and their ranges are reduced and set for the three mufflers respectively as following:

$$Obj_1(X_1, X_2, X_2) = STL(D_1, D_2, L_2) \tag{11}$$

$$Obj_2(X_1, X_2, X_3, X_4, X_5, X_6, X_7) = STL(D_1, D_2, D_3, L_1, L_2, L_3, L_5) \tag{12}$$

$$Obj_3(X_1, X_2, X_3, X_4, X_5, X_6, X_7, X_8, X_9) = STL(L_1, L_2, L_3, L_5, L_7, D_1, D_2, D_3, D_4) \tag{13}$$

4 Results and discussion

For the three studied muffler, the shape optimization is performed by testing various sets of parameters with respect to the pure tone of 300Hz. After this step, the STL is calculated with respect to various pure tones (300Hz, 500Hz, 700Hz and 800Hz) by using the optimal design obtained by optimization method.

Following the optimization process, the muffler is analyzed using a FEM and simulation analysis. The simulation analysis start by applying the required boundary conditions and then the meshing with a coarse predefined mesh sizes of 0.25mm on the x direction scale.

4.1 First case: Expansion-chamber muffler with inlet extended tube

The optimization process for the expansion chamber muffler with inlet extended tube using various sets of TA parameters is performed. The result is shown in table 2. The optimal design data is obtained at the cooling rate *CR* = 0.99 and iteration number I_{max} = 2500. This result reveals that the minimal state is achieved at the higher cooling rate.

Figure 4 plots the STL with respect to frequency in various design case. It shows that the STL values are roughly maximized at the desired frequencies and that the highest values of the *CR* and I_{max} parameters gave the highest STL. Therefore, the method of variation of these two parameters play essential role in TA optimization and using this method to find the better design solution is reliable.

The second step is to measure the STL of the optimized muffler with respect to various pure tones. Table 3 gives the obtained results of STL and this result is displayed in figure 5. This result reveals that increasing the pure tone expands the frequency bandwidth and the STLs are precisely maximized at the desired frequencies.

The 3D analysis of propagation modes is performed on the related optimal muffler's size with respect to pure tone of 2000 Hz. Figure 6 displays the internal sound pressure distribution at 2000 Hz. The pressure field varies primarily with the y direction while it is nearly constant in the z direction. The reason is that 2000 Hz is just higher than the cutoff frequency for the first symmetric propagating mode excited by the incoming wave.

We observe also that the selected frequencies how the sound pressure level distributions near the muffler inlet and outlet is important.

Table 2: Sound Transmission Loss of a single expansion-chamber muffler with targeted tone of 300 Hz and various *CR* and I_{max}.

Case	TA parameters	Results				
		R1	R2	R3	R4	STL (dB)
1	*CR* = 0.90 I_{max} = 250	0,213580756	0,202902009	0,795782821	0,781371602	20,56
2	*CR* = 0.93 I_{max} = 250	0,202115091	0,201711434	0,754368947	0,784125799	20,84
3	*CR* = 0.96 I_{max} = 250	0,201675088	0,201648677	0,759723156	0,799370566	20,96
4	*CR* = 0.99 I_{max} = 250	0,200000412	0,200000004	0,799999932	0,799993991	21,39
5	*CR* = 0.99 I_{max} = 400	0,200000297	0,2000003	0,799999879	0,798941011	21,38
6	*CR* = 0.99 I_{max} = 800	0,200002602	0,200875503	0,730584904	0,759254063	20,70
7	*CR* = 0.99 I_{max} = 1500	0,200090707	0,200030674	0,798613086	0,799459378	21,37
8	*CR* = 0.99 I_{max} = 2500	0,2	0,2	0,799999989	0,8	21,39
9	*CR* = 0.99 I_{max} = 6000	0,200000024	0,20000003	0,799999982	0,799999802	21,38
10	*CR* = 0.99 I_{max} = 10000	0,20010711	0,200000046	0,799996472	0,799834974	21,38

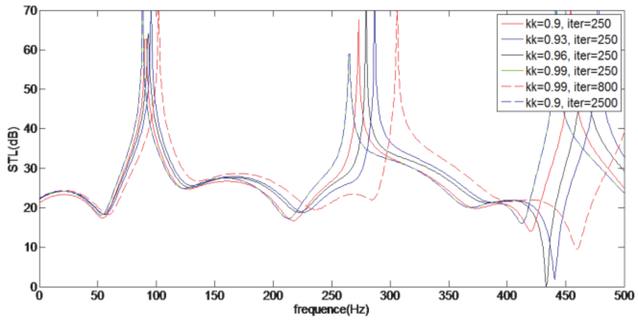

Figure 4: Performance curves of STL with respect to various maximal iterations (I_{max}) by TA [To = 0.2].

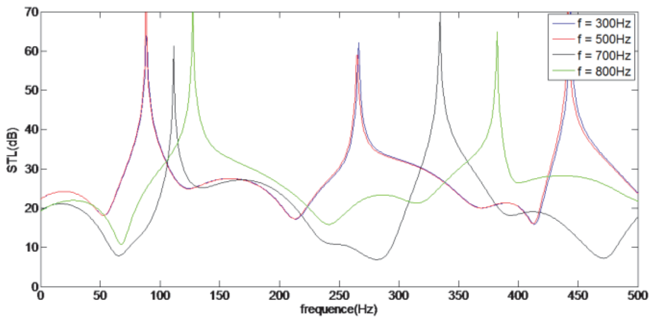

Figure 5: STL with respect to frequencies of a Single expansion-chamber for various pure tones [Targeted frequency: 300, 500, 700 and 800 Hz].

Figure 7 plots the theoretical transmission loss based on the TMM (blue line) and the FEM solution (red line) as a function of frequency. It's noticeable that the FEM solution has an upper frequency limit for its validity. This limit is the cut-on frequency which defines the frequency range where only plane waves can propagate. Above this frequency, also higher modes can propagate.

At frequencies higher than approximately 1400 Hz, the plot's behavior is more complicated and there is generally less damping. This is because, for such frequencies, the tube supports not only longitudinal resonances but also cross-sectional propagation modes. We notice that a discrepancy exists between the theoretical and the FEM solution even below the cut-on frequency. This discrepancy is due to that the elementary transfer matrices depend on the element which is modelled. The sound transmission loss is independent of the source and requires an anechoic termination at the downstream end. Thus, it does not involve neither the source nor the radiation impedance of the termination whereas the sound depend only on the sound source and does not allow the transfer matrices of the acoustic system to be obtained.

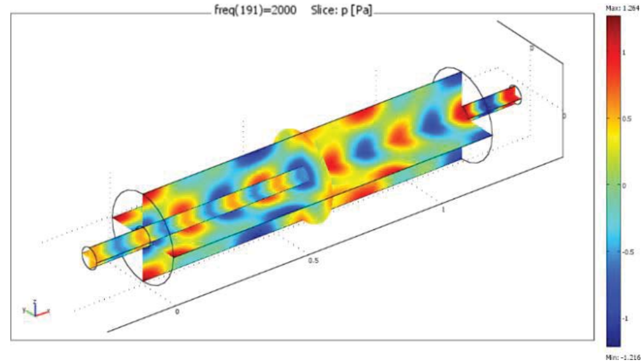

Figure 6: Optimized FEM model of the single expansion-chamber muffler with extended inlet tube and internal sound pressure distribution at 2000 Hz.

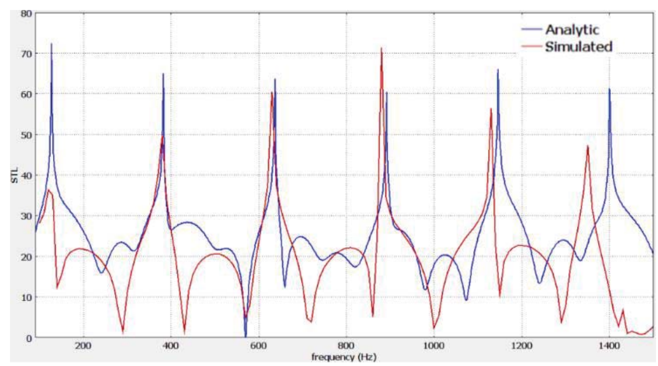

Figure 7: Muffler transmission loss versus frequency of single expansion-chamber muffler with inlet tube: Theoretical solution (blue line) and simulated solution (red line).

The differences obtained in the results may also be attributed to the finite element formulation used in simulation method which is Lagrange elements method or to the computational mesh method (density and refinement).

4.2 Second case: Expansion-chamber muffler with outlet extended tube

The shape optimization of a single expansion chamber with outlet extended tube with various sets of TA parameters with respect to the pure tone of 300Hz is performed. The result is shown in table 4.

Table 3: Sound Transmission Loss of a single expansion-chamber with respect to various targeted frequencies (CR= 0.99, I_{max} = 2500).

Case	Target frequency	Results				
		R1	R2	R3	R4	STL (dB)
1	300 Hz	0,20010935	0,20002373	0,79999829	0,79634202	22,11
2	500 Hz	0,2	0,2	0,8	0,8	25,68
3	700 Hz	0,23791322	0,46730982	0,78741544	0,64434888	115,50
4	800 Hz	0,240834641	0,200736224	0,798729653	0,555818811	119,69

Table 4: Optimal STL for a Double expansion-chamber muffler at various *CR* and I_{max} (Targeted tone of 300 Hz).

Case	TA parameters	Results				
		R1	R2	R3	R4	STL (dB)
1	$CR = 0.90$ $I_{max} = 250$	0,203970327	0,201331047	0,558524911	0,543257189	45,88
2	$CR = 0.93$ $I_{max} = 250$	0,200021583	0,200056361	0,799954532	0,792637646	49,31
3	$CR = 0.96$ $I_{max} = 250$	0,202802328	0,201578411	0,743689134	0,582243506	47,86
4	$CR = 0.99$ $I_{max} = 250$	0,200001586	0,200065207	0,799935022	0,799861406	49,34
5	$CR = 0.99$ $I_{max} = 400$	0,200181749	0,200032438	0,774090819	0,710186438	48,81
6	$CR = 0.99$ $I_{max} = 800$	0,200259589	0,200027709	0,725326708	0,798266388	48,77
7	$CR = 0.99$ $I_{max} = 1500$	0,200000723	0,200001383	0,794550818	0,79040532	49,27
8	$CR = 0.99$ $I_{max} = 2500$	0,20000004	0,200366626	0,799441375	0,799332283	49,31
9	$CR = 0.99$ $I_{max} = 6000$	0,200014056	0,20000011	0,799806204	0,798318742	49,33
10	$CR = 0.99$ $I_{max} = 10000$	0,200001007	0,200000002	0,799986738	0,799974136	49,34

As indicated, the optimal design data can be obtained at the cooling rate $CR = 0.99$ and iteration number $I_{max} = 10000$. This result indicate that the minimal state is achieved at the higher cooling rate. The acoustic performance of STL (with respect to frequency in various design case) is presented and plotted in figure 8. Obviously, the results revealed that the highest values of *CR* and I_{max} gave the highest STL. At higher frequency, the plots behavior is more complicated and the STL are roughly maximized at the desired frequencies.

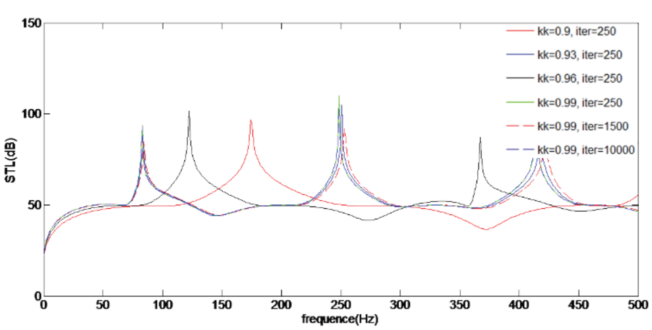

Figure 8: Performance curves of STL with respect to various maximal iterations (I_{max}) by TA [To = 0.2].

After this optimization step, the optimal design with respect to various pure tones is measured and summarized in table 5. The optimal STL curves with respect to targeted frequencies are plotted and depicted in figure 9.

The levels of the STL increase in the low frequency range whereas it decreases at high frequencies. It shows that the STLs are precisely maximized at the selected frequencies.

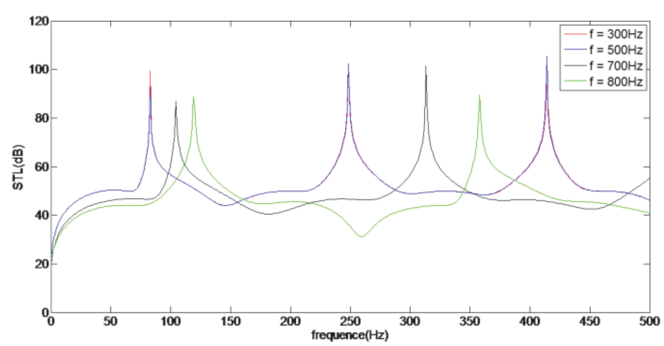

Figure 9: STL with respect to frequencies of a Double expansion-chamber muffler for various pure tones [Targeted frequency: 300, 500, 700 and 800 Hz].

Table 5: Optimal STLs for a double expansion-chamber with respect to various targeted frequencies (CR =0.95, I_{max} =50000).

Case	Targette frequency	Results				
		R1	R2	R3	R4	STL (dB)
1	300 Hz	0,200006541	0,200000986	0,799564675	0,799695519	50,09
2	500 Hz	0,2	0,2	0,8	0,8	53,64
3	700 Hz	0,236345991	0,20385864	0,653122383	0,776829314	141,22
4	800 Hz	0,212167477	0,271589061	0,797512162	0,55666418	167,92

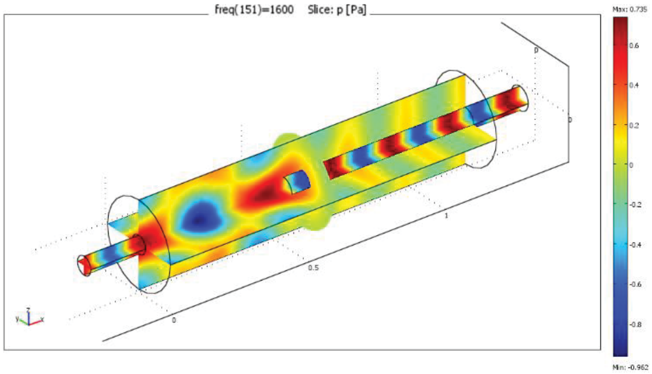

Figure 10: Optimized FEM model of the one expansion-chamber muffler and internal sound pressure distribution at 1600Hz (absolute pressure).

The 3D analysis of propagation modes is performed on the related optimal muffler's size with respect to pure tone of 1600 Hz. The result is shown in Figure 10.

We notice that for the selected frequencies how the sound pressure level distributions near the muffler outlet is important.

Figure 11 plots the theoretical transmission loss (blue line) and the numerical solution (red line) as a function of frequency. We observe a discrepancy between the analytic and the simulated plots is higher than those of muffler with inlet extended tube. Also we notice that the FEM solution present an upper frequency limit for its validity which is around 1500 Hz. This limit is the cut-on frequency defined previously.

4.3 Third case: Expansion-chamber muffler with inlet and outlet extended tube

The result of the shape optimization of a the expansion-chamber muffler with inlet and outlet extended tubes based on various sets of TA parameters and with respect to the pure tone of 300Hz is shown in table 6.

As indicated, the optimal design data can be obtained at the cooling rate CR = 0.99 and iteration number I_{max} = 10000. It reveals that the minimal state is achieved at the higher cooling rate. The acoustic performance of STL (with respect to frequency in various design case) is presented and plotted in figure 12.

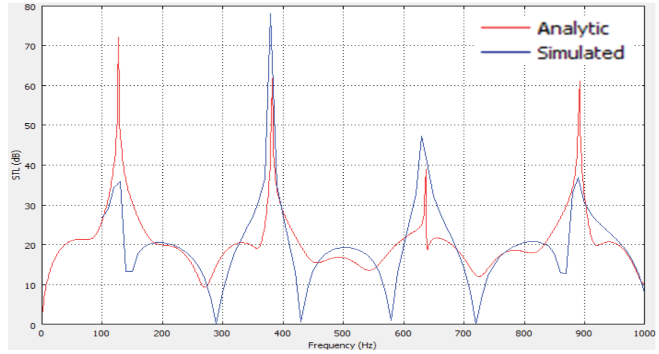

Figure 11: Single expansion-chamber muffler with outlet extended tube, transmission loss versus frequency (Theoretical solution (blue line) and simulated solution (red line)).

Obviously, the results reveal that the highest values of the maximum of (CR and I_{max}) gave the highest STL. At higher frequency, the plots behavior is more complicated and the STLs are roughly maximized at the desired frequencies. The STL of the muffler's optimal sizes with respect to various pure tones are summarized in table 7. The optimal STL curves with respect to targeted frequencies are plotted and depicted in figure 13. We notice that the levels of the transmission loss increase in the low frequency range, whereas the levels decrease at high frequencies and it shows that the STLs are precisely maximized at the selected frequencies. After that the 3D analysis of propagation modes is performed on the related optimal muffler's size with respect to pure tone of 2820 Hz.

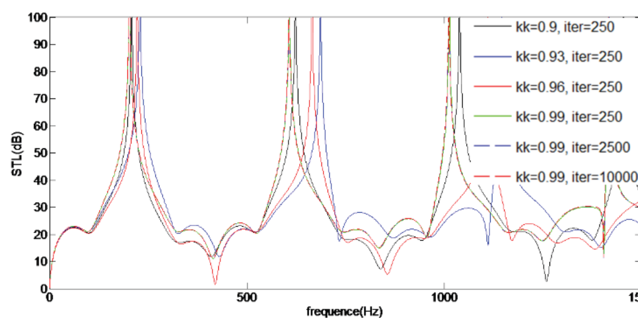

Figure 12: Performance curves of STL with respect to various maximal iterations (I_{max}) by TA [To = 0.2].

Table 6: Optimal STL for a Double expansion-chamber muffler at various CR and I_{max} (Targeted tone of 300 Hz).

Case	TA parameters	Results				
		R1	R2	R3	R4	STL (dB)
1	CR = 0.90, I_{max} = 250	0,493648572	0,200000002	0,7995986	0,318039144	21,31
2	CR = 0.93, I_{max} = 250	0,20040704	0,200000006	0,799314016	0,380509568	21,38
3	CR = 0.96, I_{max} = 250	0,49057417	0,200938109	0,796665887	0,358804594	21,11
4	CR = 0.99, I_{max} = 250	0,203700732	0,200000011	0,793509973	0,302309052	21,62
5	CR = 0.99, I_{max} = 400	0,202774242	0,200670458	0,779143091	0,355654907	21,29
6	CR = 0.99, I_{max} = 800	0,200927913	0,200172399	0,799162089	0,30012868	21,65
7	CR = 0.99, I_{max} = 1500	0,200775342	0,2	0,79999581	0,301296387	21,67
8	CR = 0.99, I_{max} = 2500	0,200003813	0,2	0,799782514	0,300023475	21,67
9	CR = 0.99, I_{max} = 6000	0,200037701	0,200000069	0,799983124	0,30018866	21,67
10	CR = 0.99, I_{max} = 10000	0,2	0,2	0,799999999	0,3	21,68

Table 7: Optimal STLs for a double expansion-chamber with respect to various targeted frequencies (CR=0.95, I_{max} =50000).

Case	Targette frequency	Results				
		R1	R2	R3	R4	STL (dB)
1	300 Hz	0,200378869	0,200005517	0,799887167	0,300417339	22,49
2	500 Hz	0,200004147	0,200002545	0,61423464	0,300032686	23,14
3	700 Hz	0,200428366	0,200205034	0,799994563	0,300055346	23,25
4	800 Hz	0,20000481	0,20001244	0,799999553	0,300006166	28,62

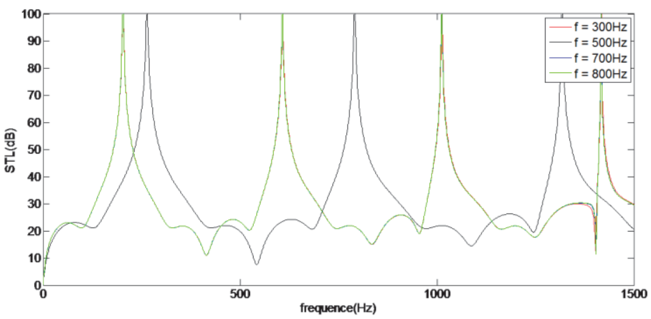

Figure 13: STL with respect to frequencies of the expansion-chamber muffler with inlet and outlet extended tube for various pure tones [Targeted frequency: 300, 500, 700 and 800 Hz].

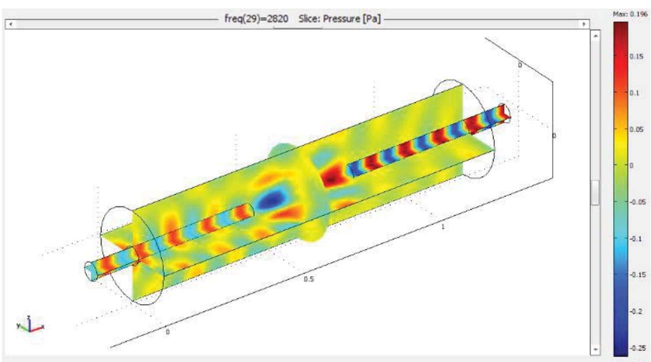

Figure 14: Optimized FEM model of the one expansion-chamber muffler and internal sound pressure distribution at 2820Hz (absolute pressure).

Figure 14 shows the internal sound pressure distribution at 2820 Hz of the single expansion chamber muffler, we observe how the sound pressure level is higher than those of muffler with inlet extended tube and outlet extended tube in high frequencies. We can also observe for the selected frequencies how the sound pressure level distributions near the muffler outlet is important.

Figure 15 plots the theoretical transmission loss (blue line) and the simulation solution (red line) as a function of frequency.

The FEM solution has an upper frequency limit for its validity. This limit is the cut-on frequency defined previously, we observe a discrepancy between the analytic and the simulated plots as the theoretical results based on the TMM depend on the element which is modelled and not on the source whereas the FEM solution is based on the sound acoustic power method and depend only on the sound source and do not allow the transfer matrices of the acoustic system to be obtained.

The discrepancy obtained in the results plot may also be attributed to the used formulation in finite element method which is Lagrange elements or to the computational meshed applied (density and refinement).

4.4 Comparison

The optimal muffler's design data for the three kinds of expansion-chamber mufflers with extended tubes (inlet, outlet and inlet/outlet tubes) with space constraint is summarized in table 8 and plotted in figure 16. As shown, it is obvious that the attenuation of the single expansion-chamber muffler with inlet and outlet tube is a little superior to the other mufflers. Consequently it gives the best acoustical performance.

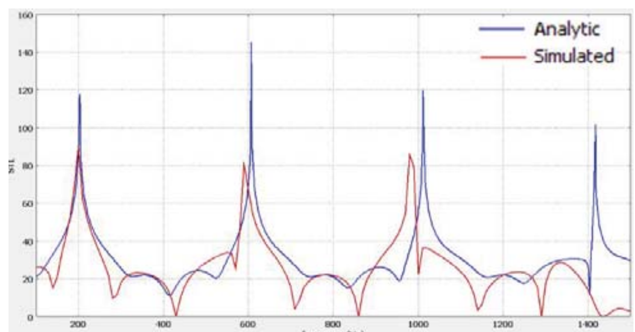

Figure15: Expansion-chamber muffler with inlet and outlet extended tube transmission loss versus frequency: theoretical solution (blue line) and simulated solution (red line).

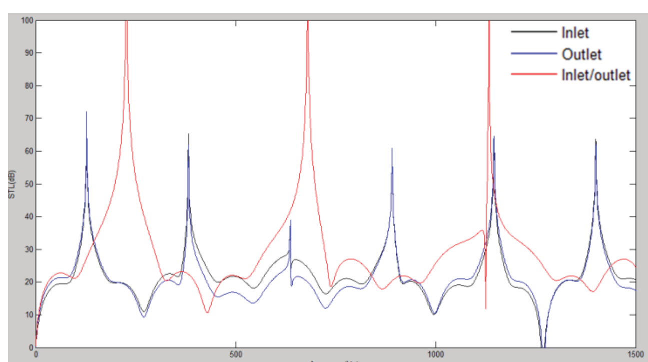

Figure 16: Comparison of the optimal STL level with respect to the three kinds of optimized mufflers within a same space-constrained space [broadband noise].

Table 8: Comparison of the acoustical performance with respect to three kinds of optimized mufflers within same space-constrained situation.

Case	Type of muffler	Results				
		R1	R2	R3	R4	STL (dB)
1	Inlet extended tube	0,24	0,2	0,79	0,55	119,69
2	Outlet extended tube	0,21	0,27	0,79	0,55	167,92
3	Inlet & Outlet extended tubes	0,2	0,2	0,79	0,3	28,62

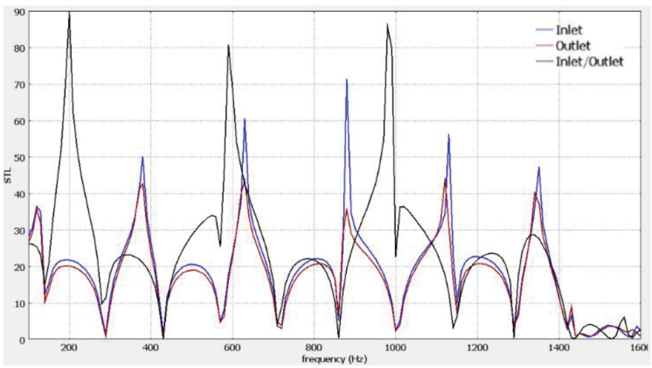

Figure 17: FEM solution of the three shape optimized mufflers: Inlet (Blue line), Outlet (Red line) and Inlet/Outlet (Black line).

For the FEM Solution, the sound attenuation of the three optimized mufflers' configurations as a function of frequency is plotted in figure 17. The plot shows that for the muffler with inlet and outlet extended tubes gives the highest acoustical performance than the two other mufflers.

5 Conclusion

The shape optimization of three kinds of reactive mufflers with extended tubes under space constraints is applied in this paper by using a novel scheme Threshold Acceptance coupled with 3D finite element analysis.

This numerical analysis using TA optimizer shows to be an efficient method to optimize reactive mufflers under space constraints.

The TA optimizer is based on the TMM method applying the plane wave theory as well as four-pole transfer matrices. This optimization method shows the importance of the two TA parameters (*CR* and I_{max}) in the optimization process also it reveals that this method is valid when the influence of high order modes can be neglected. For the FEM, the analysis is performed on the shape optimized mufflers obtained by the TA methods. This method depend on the sound acoustic power. The TMM depends on the element which is modelled and not on the sound source, whereas for the sound acoustic power depend on the sound source and does not allow the transfer matrices of the acoustic system to be obtained, also it depends on the finite element formulation and the computational mesh method.

The comparison between the numerical prediction based on the TMM and the FEM solution based on the sound acoustic power displays higher discrepancies in the curves for the muffler with outlet extended tube than the two other mufflers.

The TA optimization method and the FEM method showed that the single expansion-chamber muffler with inlet and outlet extended tube provides considerably better STL values than the two other mufflers.

Consequently, the approach of the optimal design of STL proposed in this study is quite efficient in dealing with the reactive mufflers within a space-constrained situation.

Acknowledgments

The authors acknowledge the support given by the technology department and mechanical engineering department of the University of Bejaia.

References

[1] E. Bécache, A.S. Bonnet-Bendhia, Numerical simulation of exhaust muffler, An homogenized finite element method, Cari'06, Vol. 1, (2006), pp. 1-10.

[2] S. Bilawchuk, K. R. Fyfe, Comparison and implementation of the various numerical methods used for calculating transmission loss in silencer systems, Appl. Acoust. , Vol. 64, (2003), pp. 903-916.

[3] S.N.Y. Gerges, R. Jordan, F.A. Thime, J.L. Bento Coelho, J.P. Arenas, Muffler Modeling by Transfer Matrix Method and Experimental Verification, J. Braz. Soc. Mech. Sci.& Eng., Vol. 27(2), (2005), pp. 132-140.

[4] M.L. Munjal, Plane wave analysis of side inlet/outlet chamber mufflers with mean flow, Appl. Acoust. , Vol. 52(2), (1997), pp. 165-175.

[5] M. L. Munjal, Acoustics of Ducts and Mufflers with Application to Exhaust and

Ventilation System Design, John Wiley & Sons, Inc., (1987), pp. 328.

[6] M. L. Munjal, Advances in the acoustics of flow ducts and mufflers, Vol. 15(2), (1990), pp. 57-72.

[7] K.S. Andersen, Analyzing Muffler performance using the Transfer Matrix Method, Proc.Comsol Conf., (2008).

[8] L.J. Yeh, M.C. Chiu, Computer aided design on single expansion muffler under space constraints, Proc. 19th Nat. Conf. Mech. Eng., Vol. C7, (2002) pp. 625-633.

[9] R.J. Bernhard, Shape Optimization of Reactive Mufflers, Noise Cont Eng J, Vol. 27(1), (1986) pp. 10-17.

[10] M.C. Chiu, L.J. Yeh, Shape Optimization of Single-Chamber Mufflers with Side Inlet/Outlet by Using Boundary Element Method, Mathematic Gradient Method and Genetic Algorithm, Tamkang J. Sc. Eng., Vol. 12(1), (2009) pp. 85-98.

[11] L.J. Yeh, Y.C. Chang, M.C. Chiu, Shape Optimal Design on Double-Chamber Mufflers Using Simulated Annealing and a Genetic Algorithm, Turkish J. Eng. Env. Sc., Vol. 29, (2005), pp. 207- 224.

[12] P. W. Jones, N. J. Kessissoglou, Experimental study of the Transmission Loss of Mufflers used in Reperatory Medical Devices, Vol. 38, (2010) , pp. 1 - 13

[13] M.L. Munjal, A. G. GALAITISIS, I. L. VER, Passive Silencer, Noise Vibration Control Engineering, J. Wiley & Son, Inc., (2005), pp. 279-343.

[14] Davies, P.O.A.L., Realistic Models for Predicting Sound Propagation in Flow Duct Systems, Noise Cont. Eng. J. , Vol. 40,(1993), pp. 135-141. [18]

[15] Beranek, L.L, Istvan, L, Noise and Vibration Control Engineering: Principles and Applications, John Wiley & Sons, Inc, (1992), ISBN 0-471-61751-2.

[16] O. Bräysyean, J. Berger, A Threshold Accepting Metaheuristic for the Vehicle Routing Problem with Time Windows, Appl. Math., (2003).

[17] A. Metropolis, Rosenbluth, Equation of static calculations by fast computing machines, J. Chem. Phys., Vol. 21(6), (1953), pp. 1087-1092.

[18] G. Dueck, T. Scheurer, Threshold accepting: A general purpose optimization algorithm appearing superior to simulated annealing, J. Comput. Phy., vol. 90, (1990), pp. 161-175.

[19] M. Yagiura, T. Ibaraki, On metaheuristic algorithms for combinatorial optimization problems, Sys. Comp. Japan, vol. 32, (2001), pp. 33–55.

[20] COMSOL 3.4, Acoustics Module Model Library, COMSOL AB, (2007), pp. 74-85.

Notation

STL	Sound transmission loss (dB)
w_i	time-averaged incident sound power
w_t	transmitted sound power
q	dipole source
p_0	incoming pressure wave
k_1	wave vector
I	time-averaged sound intensity
W	transmitted sound powers
c_0	sound speed (m/s)
D_0	diameter of the expansion chamber in the muffler (m)
D_i	diameter of the i-th segment of the muffler (m)
f_{01}	cut-off frequency (Hz)
f	cyclic frequency (Hz)
I_{max}	maximum iteration
j	imaginary unit
k	wave number
CR	cooling rate in SA
L_0	total length of the muffler (m)
L_i	length at the i-th element (m)
M_i	mean flow Mach number at the ith element
Obj_i	objective function (dB)
p	acoustic pressure (Pa)
p_i	acoustic pressure at the ith node (Pa)
u	acoustic particle velocity (ms^{-1})
u_i	acoustic particle velocity at the *ith* node ($m\ s^{-1}$)
ρ_0	air density ($kg\ m^{-3}$)
$pb(T)$	transition probability
To	initial temperature (°C)
Q	volume flow rate of venting gas ($m^3\ s^{-1}$)
S_i	section area at the i-th node (m^2)